

Supplemental Figure 1

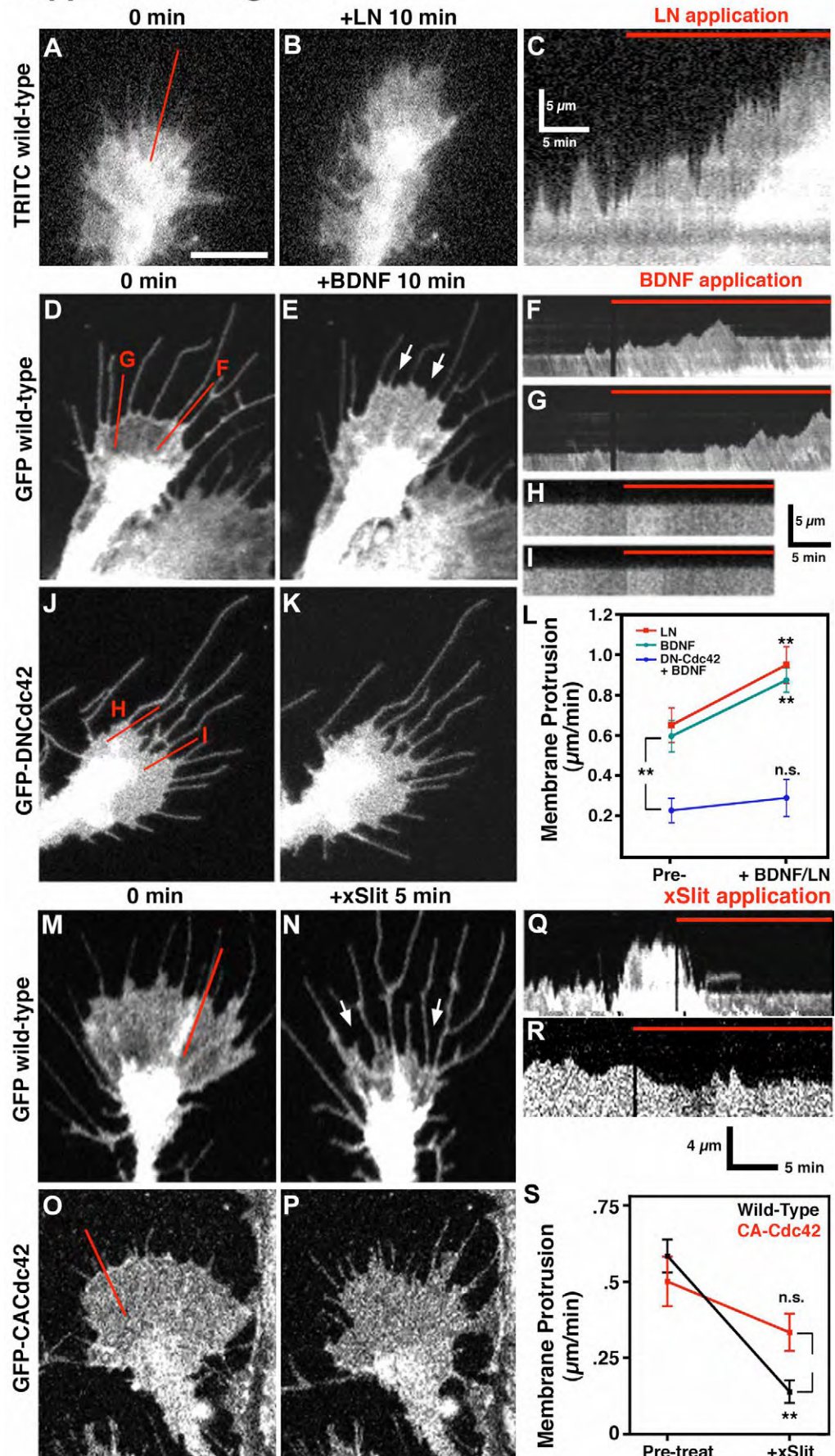


Fig. 1. BDNF and LN promote and Slit inhibits protrusion through Cdc42. (A,B) Fluorescence images of a TMR-D loaded growth cone at times indicated during LN application. (C) Single line kymograph of region indicated by red line in (A). Note an increase in the stability of protrusions 5 min after LN addition. (D,E). GFP-expressing growth cone at times indicated during BDNF application. Note expanding area due to lamellipodial protrusion at the leading edge (arrows). (F,G) Single line kymographs of regions indicated by red lines in (D). Note that the region sampled by line F becomes protrusive immediately after BDNF application, whereas the region sampled by line G becomes active after a delay of approximately 10 min. (J,K). A GFP-DNCdc42 expressing growth cone at times indicated during BDNF application. Note that this growth cone undergoes little change in morphology after 10 min in BDNF. (H,I). Single line kymographs of regions indicated by red lines in J. Neither region exhibits a detectable increase in membrane protrusion any time after BDNF application. (L) Quantification of the effects of BDNF or LN on total membrane protrusion in wild-type TMR-D loaded, GFP and GFP-DNCdc42 expressing growth cones. The extent of protrusion was analyzed for 0-10 min before and 5-15 min following BDNF addition. N=20 for each condition. *P<0.05, **P<0.001. M-N. Fluorescence images of a GFP-expressing wild-type growth cone before and after xSlit application. Note reduced growth cone area as a result of lamellipodial retraction at the leading edge (arrows). (O,P) A GFP-CACdc42 expressing growth cone before and after xSlit application. Note partial retraction of growth cone lamellipodia following the addition of xSlit (arrow). (Q,R) Single line kymographs of regions sampled by red lines in M and O. In the control growth cone, the lamellipodial retracts and protrusive activity ceases after xSlit addition (Q). In contrast, the region sampled from the CACdc42-expressing growth cone retains some protrusive activity following xSlit stimulation (R). (S) The effects of xSlit on total membrane protrusion in wild-type GFP and GFP-CACdc42 expressing growth cones. The extent of protrusion was analyzed for 0-10 min before and 2-12 min following xSlit addition. N≥12 for each condition. **P<0.001 by Students t-test. Scale bar, 5 μm.

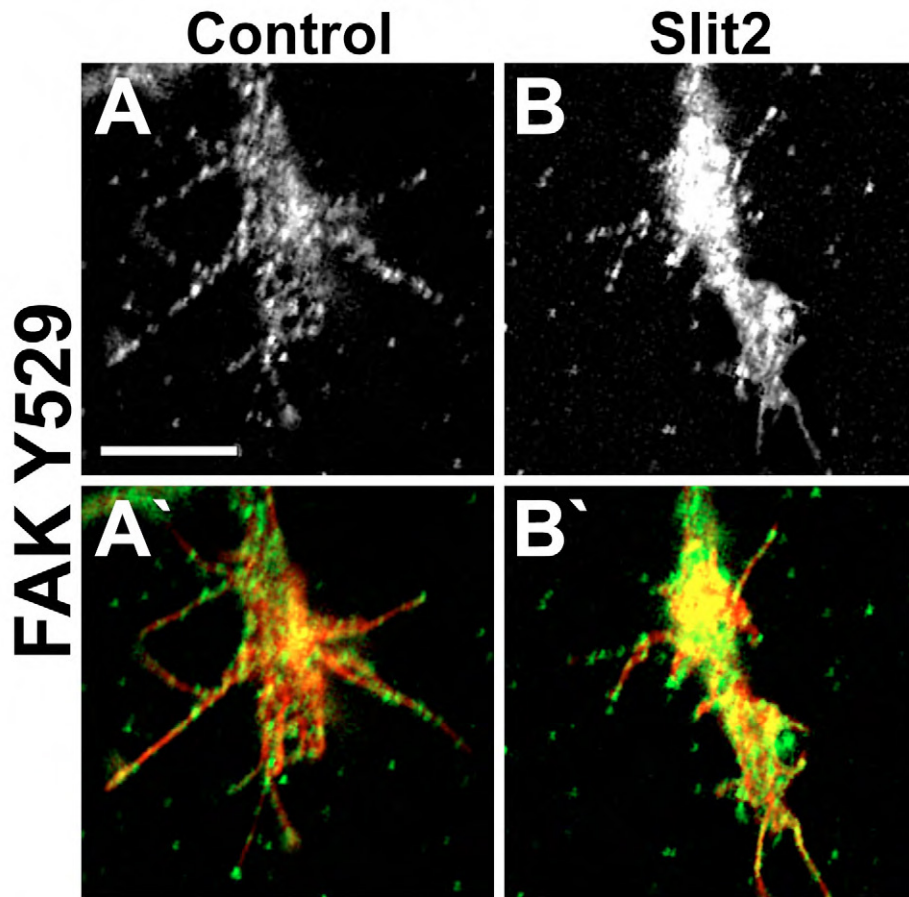
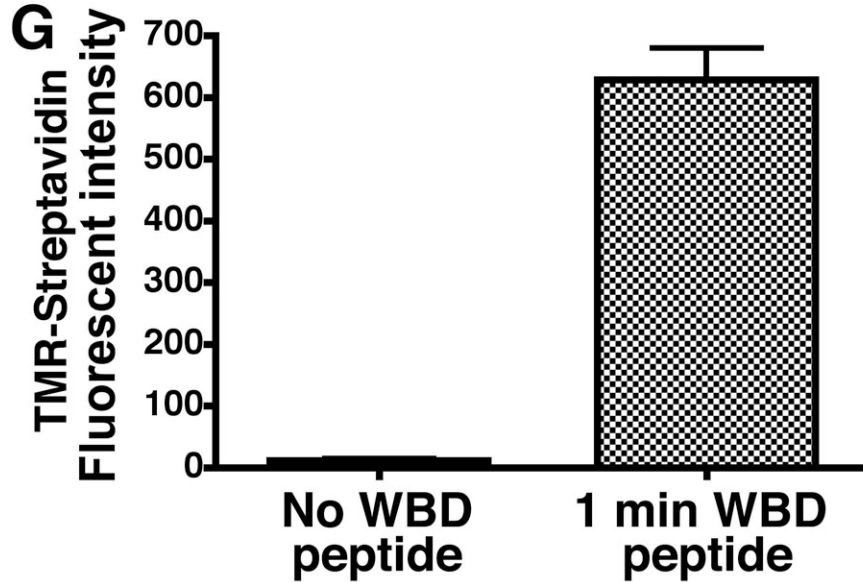
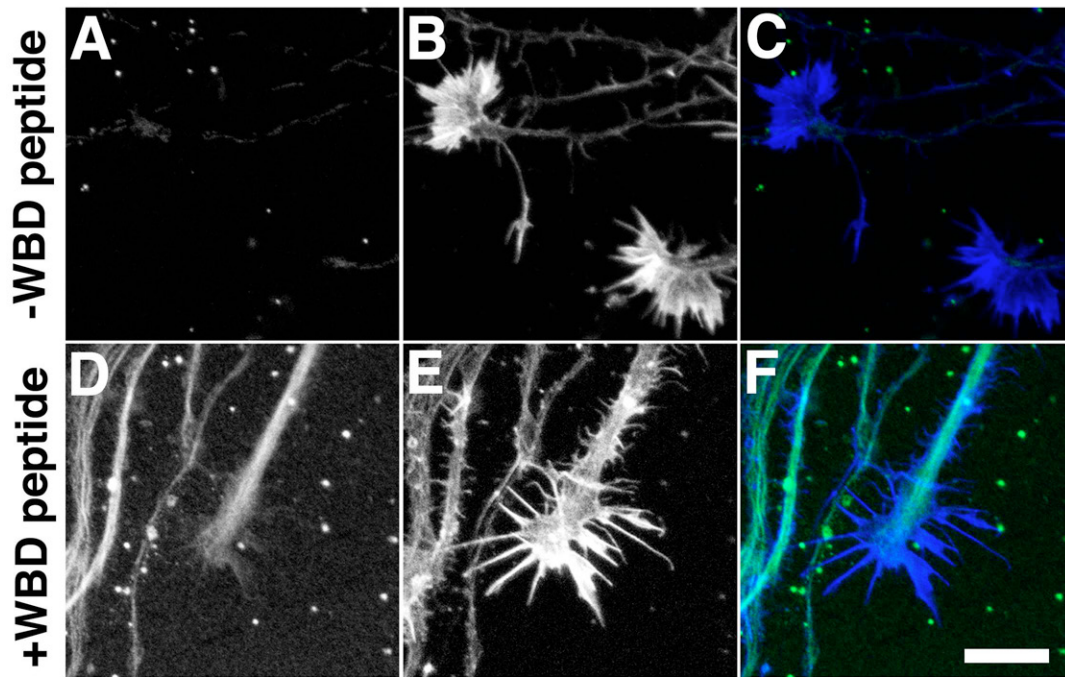


Fig. 2. Slit2 inactivates FAK and Src in neurons cultured on LN. (A,B) Control and Slit2-treated neurons on LN, fixed and stained with phospho-specific antibodies against Y529 Src. (A',B') Merged images of immunolabeled growth cones in A, B (green) merged with f-actin (red). Note increased labeling of phospho Y529 Src, suggesting inactivation of Src by Slit2. Scale bar, 5 μ m.



Supplemental Figure 3. Rapid loading of WBD-CRIB peptide into growth cones. (A,B) TMR-streptavidin labeling (A) and Alexa-647 phalloidin stained (B) single channel fluorescence images of untreated control neurons. C. Pseudocolored merged images of TMR-streptavidin (green) and phalloidin (blue) growth cones from (A,B). D, E. TMR-streptavidin labeling (D) and Alexa-647 phalloidin stained (E) single channel fluorescence images of neurons treated with 40 µg/ml WBD-CRIB-biotin for 1 min. F. Pseudocolored merged images TMR-streptavidin (green) and phalloidin (blue) growth cone from (D, E). Note strong TMR-streptavidin labeling of growth cone and axons in (D) indicating WBD-CRIB-biotin loaded into neurons, but no labeling of neurons in (A). (G) Quantitative fluorescence intensity measurements of TMR-streptavidin labeling of untreated control growth cones and growth cones treated with 40 µg/ml WBD-CRIB-biotin for 1 min. N=10 growth cones for each condition. $P < 0.0001$, Students t-test. Scale bar, 10 µm.

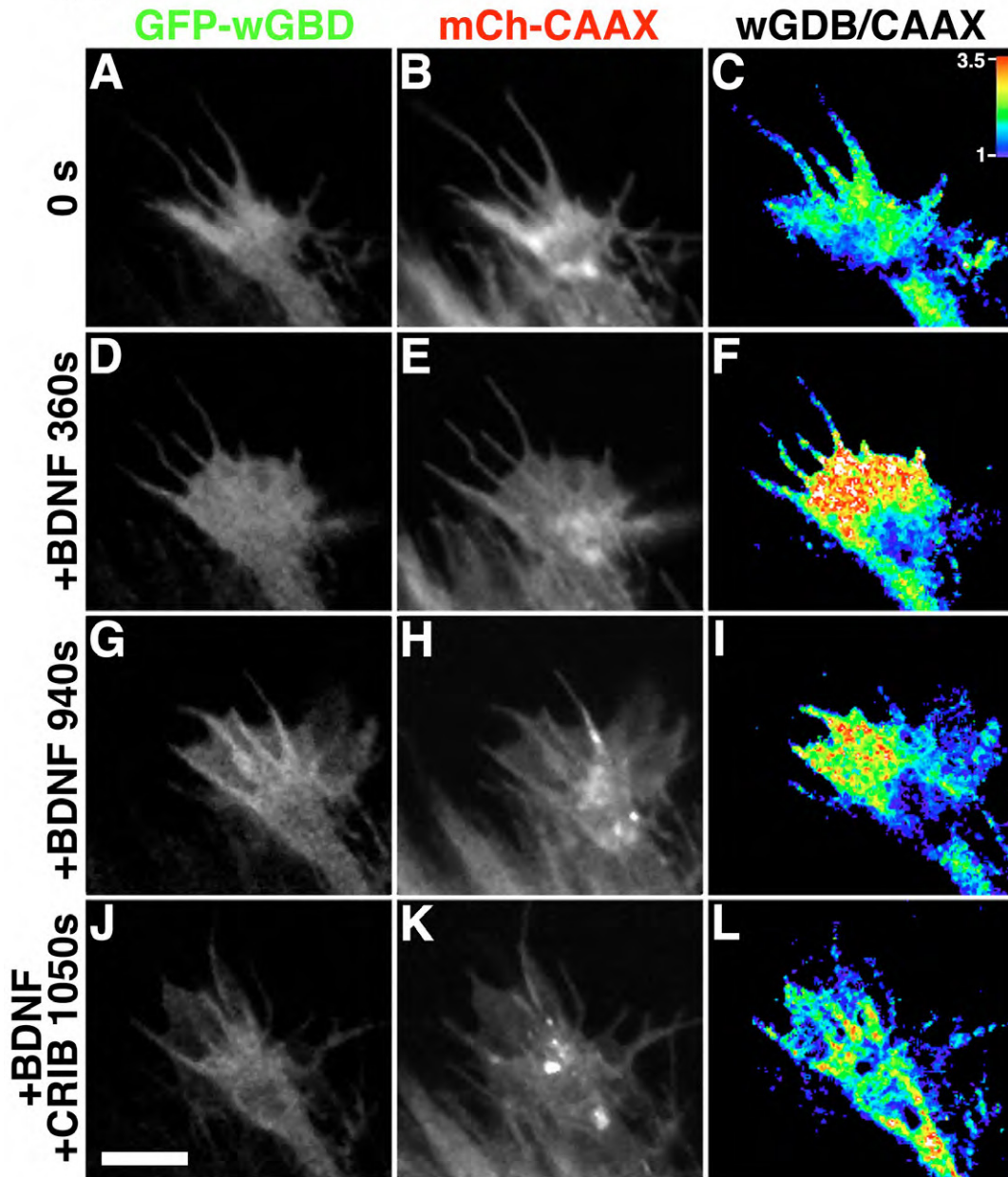


Fig. S4. Live imaging of Cdc42 activity in growth cones using GFP-wGBD and mCherry-CAAX. (A, B) GFP-wGBD and mCherry-CAAX (mCh-CAAX) single channel fluorescence images of a growth cone on PDL before BDNF stimulation. (C) GFP-wGBD/mCh-CAAX ratio image of growth cone in (A,B). Note that the intensities of individual fluorescence images in this figure were contrast enhanced to highlight the growth cone morphology, but ratio images were created from raw images. (D-F) Single channel and fluorescence ratio images 360 seconds following BDNF application. Note a robust increase in the wGBD/mCh-CAAX ratio is apparent at the growth cone periphery by 360 seconds following stimulation. (G-I) Single channel and fluorescence ratio images 940 seconds following BDNF application and just before addition of the CRIB-peptide. Note that active Cdc42 remains elevated for over 15 minutes, although dampened slightly. (J-L) Single channel and fluorescence ratio images 1050 seconds following addition of 40 μ g/ml N-WASP CRIB-peptide together with BDNF. Within 2 minutes of CRIB-peptide addition, active Cdc42 is dramatically reduced at the periphery, which corresponds precisely with reduced protrusive activity. Pseudocolor scale in C applies to C, F, I and L. Scale bar, 5 μ m.

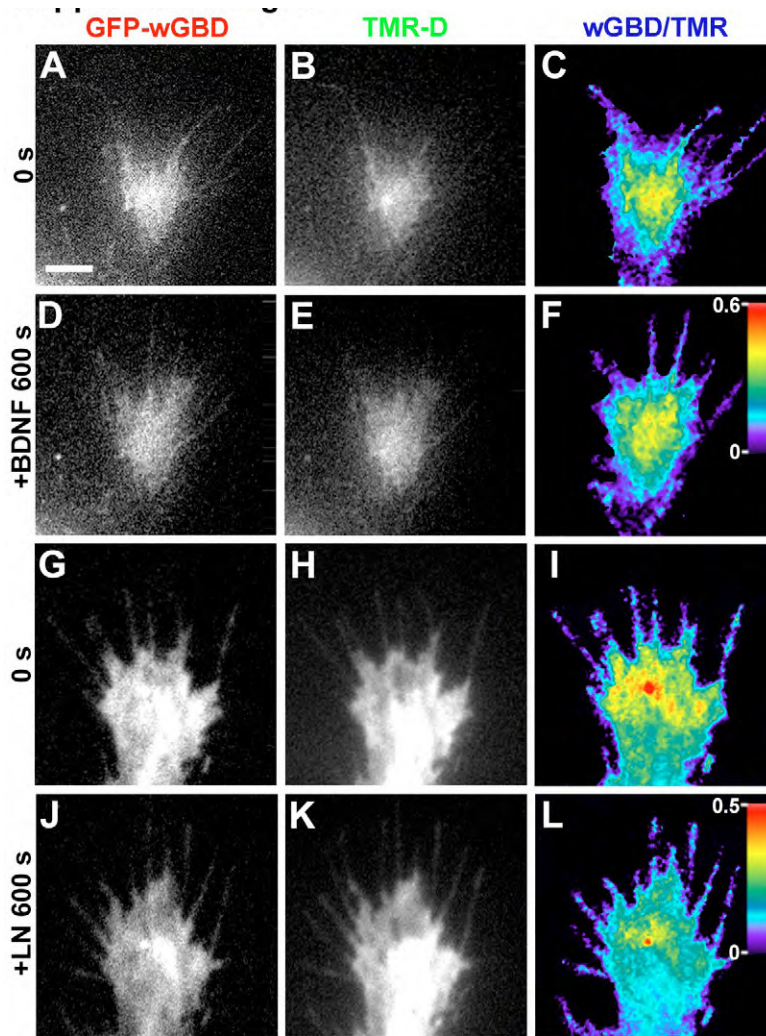


Fig. S5. Cdc42 activity is not elevated by BDNF or LN in FRNK expressing growth cones. (A,B) GFP-wGBD and TMR-D single channel fluorescence confocal images of a growth cone on PDL before BDNF stimulation. Note that for display purposes, some individual images were contrast enhanced, but ratio images were generated from raw images. (C) GFP-wGBD/TMR-D ratio image of growth cone in (A and B). (D-F) Single channel and fluorescence ratio images 600 seconds following application of BDNF to FRNK expressing growth cones. Note little change in the wGBD/TMR-D ratio is apparent at the growth cone periphery by 600 seconds following stimulation. (G,H) GFP-wGBD and TMR-D single channel fluorescence confocal images of a growth cone on PDL before LN stimulation. (I) GFP-wGBD/TMR-D ratio image of growth cone in (G and H). (J-L) Single channel and fluorescence ratio images 600 seconds following application of LN to FRNK expressing growth cones. Note little change in the wGBD/TMR-D ratio is apparent at the growth cone periphery by 600 seconds following stimulation. Scale bar, 5 μ m.

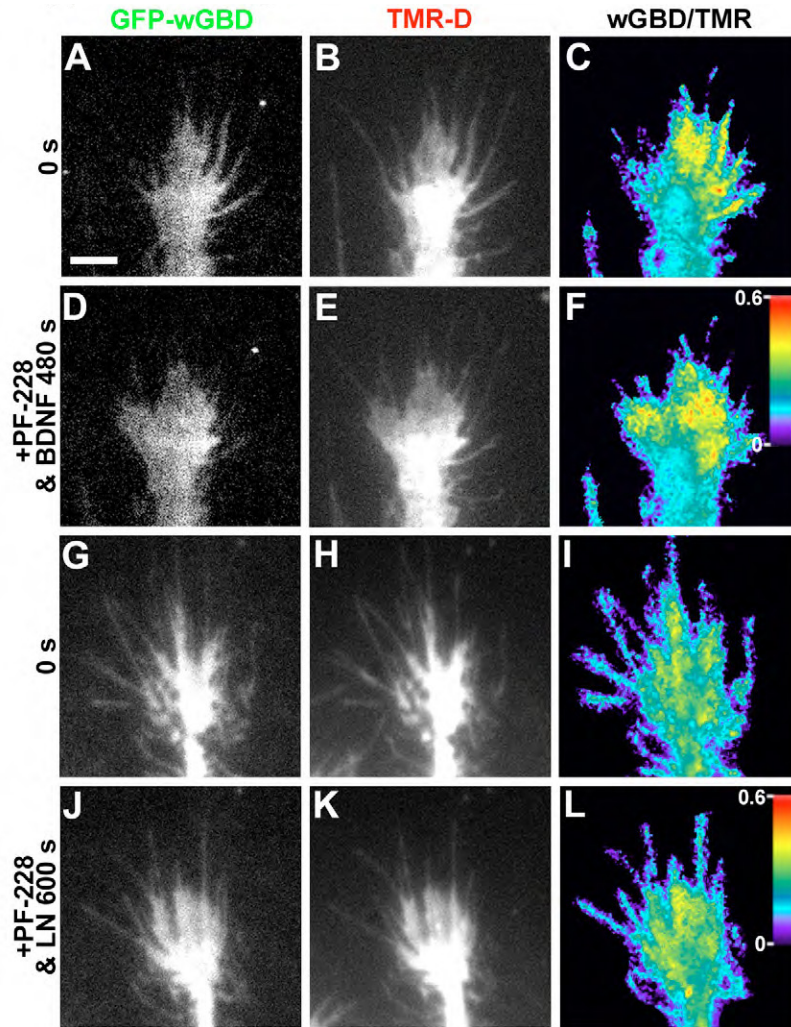


Fig. 6. Cdc42 activity is not elevated by BDNF or LN when FAK is inhibited with PF-228. (A,B) GFP-wGBD and TMR-D single channel fluorescence confocal images of a growth cone on PDL before BDNF stimulation. Note that for display purposes, some individual images were contrast enhanced, but ratio images were generated from raw images. (C) GFP-wGBD/TMR-D ratio image of growth cone in (A and B). (D-F) Single channel and fluorescence ratio images 480 seconds following simultaneous addition of 100 nM PF-228 and BDNF. Note little change in the wGBD/TMR-D ratio is apparent at the growth cone periphery by 480 seconds following stimulation. (G,H) GFP-wGBD and TMR-D single channel fluorescence confocal images of a growth cone on PDL before LN stimulation. I. GFP-wGBD/TMR-D ratio image of growth cone in (G and H). (J-L) Single channel and fluorescence ratio images 600 seconds following simultaneous addition of 100 nM PF-228 and LN. Note little change in the wGBD/TMR-D ratio is apparent at the growth cone periphery by 600 seconds following stimulation. Scale bar, 5 μ m.

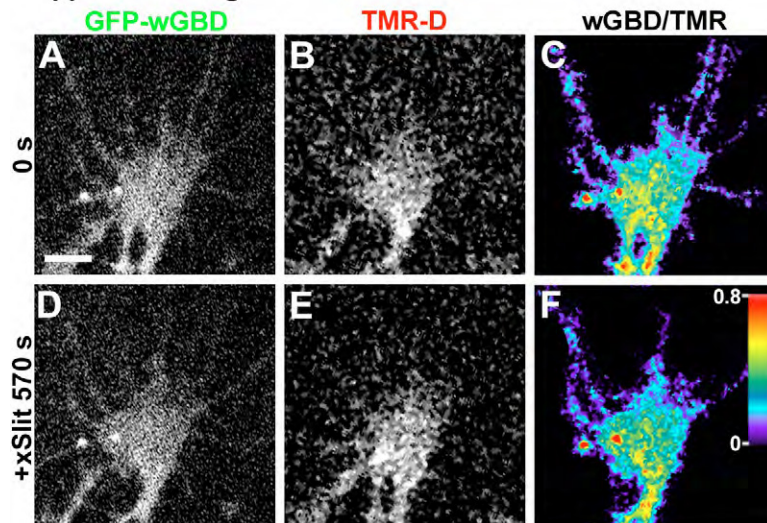


Fig. S7. Slit2 inhibition of Cdc42 is blocked by constitutively active FAK. (A,B) GFP-wGBD and TMR-D single channel fluorescence confocal images of a SuperFAK expressing growth cone on PDL before Slit stimulation. Note that for display purposes, some individual images were contrast enhanced, but ratio images were generated from raw images. (C) GFP-wGBD/TMR-D ratio image of growth cone in (A and B). (D-F) Single channel and fluorescence ratio images of a SuperFAK expressing growth cone 570 seconds following Slit addition. Note little change in the wGBD/TMR-D ratio is apparent at the growth cone periphery by 570 seconds following stimulation. Scale bar, 5 μ m.